Journal of KSNVE, Vol. 8, No. 5, pp. 974~980, 1998.

〈Original Paper〉

Dynamic Responses on Semi-Infinite Space Due to Transient Line Source in Orthotropic Media

선형하중에 의한 직교이방성 매체의 반구계에서 동적 응답 특성

Yong-Yun Kim*
김 용 연

(Received June 25, 1998 ; Accepted September 2, 1998)

Key Words : Transient LineLoad (순간선형하중), Orthotropic Media(직교이방성 매체), Surface Wave (표면파) , Semi-Infinite Space(반구계)

ABSTRACT

The analysis of dynamic responses are carried out on several orthotropic systems due to transient line source. These include infinite and semi-infinite spaces. The media possess orthotropic or higher symmetry. The load is in the form of a normal stress acting with parallel to symmetry axis on the plane of symmetry within the materials. The results are first derived for responses of infinite media due to a harmonic line source. Subsequently the results for semi-infinite are derived by using superposition of the solution in the infinite medium together with a scattered solution from the boundaries. The sum of both solutions has to satisfy stress free boundary conditions thereby leading to the complete solutions. Explicit solutions for the displacements due to transient line loads are then obtained by using Cargniard-DeHoop contour.

요 약

본 논문은 직교이방성 탄성계에서 내부 선형하중에 의한 탄성파의 거동을 고찰하였다. 첫째로, 내부 발진원에 대한 탄성파 거동식을 무한계와 반구계의 직교이방성 매체에서 유도하였고, 둘째로 Cargniard-DeHoop을 이용하여 순간선형하중에 대한 무한계와 반구계에서의 탄성파 거동식을 유도하였다. 반구계에서 탄성파에 대한 거동식은 무한계에서 유도한 결과와 반구의 표면에서 분산되는 반사파의 합으로 표현되고, 경계영역에서 경계조건을 만족하였다. 여러 가지 이방성 매체에 대한 수치해석 결과를 제시하였고, 이방성 매체의 특성인 bulk wave의 Lacunae 및 표면파의 영향을 고찰할 수 있었다. 본 논문의 결과는 지진연구, 복합소재 특성 연구, 지능형소재 특성연구 등에 응용될 것이다.

1. Introduction

Acoustic vibrations in solid structures essentially involve the propagation of wave motion throughout the supporting media. In dealing with acoustic vibrations of systems involving coupling of compressible fluids with plate and shell

* 정회원, 삼성항공산업(주), 정밀기기연구소

structures, it is important to possess an appreciation of the "wave view" of vibration. Thus, understanding the response of elastic solids to internal mechanical sources has long been of interest to researchers in classical fields such as acoustics, vibration, seismology, as well as modern fields of application like ultrasonics and acoustic emission.

Elastic wave interactions with homogeneous elastic anisotropic media, in general, and with layered anisotropic media, in particular, have been extensively investigated in the past decade or so. This advancement has been prompted at least from a mechanics point of view, by the increased use of advanced composite materials in many structural applications. The effect of imposed line load in homogeneous isotropic media has been discussed by several investigators ever since Lord Rayleigh discovered the existence of surface waves on the surfaces of solids[12]. An account of the literature dealing with this problem through 1957 can be found in Ewing, Jardetzky and Press[8]. Most of the earlier works [8~10] followed Lamb[11], who apparently was the first to consider the motion of half space caused by a vertically applied line load on the free surface or within the isotropic medium. He was able to show that displacement at large distance consist of a series of events which correspond to the arrival of longitudinal, shear, and Rayleigh surface wave. For a transient source loading results can be obtained from those corresponding to harmonic ones by a Fourier integral approach. The resulting double integral could be evaluated only by considering large distance. However, a suitable deformation of the integral contour by Cargniard-DeHoop not only resulted in considerable analytical simplification but led to exact, closed algebraic espression for the displacement of time[7].

In this paper, the formal developments in previous works are rigorously followed[1~4] and study the response of several anisotropic systems due to buried transient line loads. These include infinite and semi-infinite, structures. The problem is mathematically formulated based on the equations of motion in the constitutive relations. The internal line load will be in the form of a normal stress load, acting at a symmetry direction within the materials in the plane of symmetry. The load is first described as a body force in the equations of the motion for the infinite media and then it is mathematically characterized as "artificial interface conditions" for each semi-infinite spaces. A building block approach is utilized in which the analysis has begun by deriving the results for an infinite media. Subsequently the results for semi-infinite spaces, by using superposition of the infinite medium solution together with a scattered solution from the free surface. The sum of both solutions has to satisfy the stress free boundary conditions, thereby leading to a complete solution. Consequently explicit solutions for the displacements are obtained by using Cargniard-DeHoop contour.

2. Problem Formulation

Consider an infinite anisotropic elastic medium possessing orthotropic symmetry. The medium is oriented with respect to the reference cartesian coordinate system $x_i=(x_1,x_2,x_3)$ such that the x_3 is assumed normal to its plane of symmetry as shown in Fig. 1. The plane of symmetry

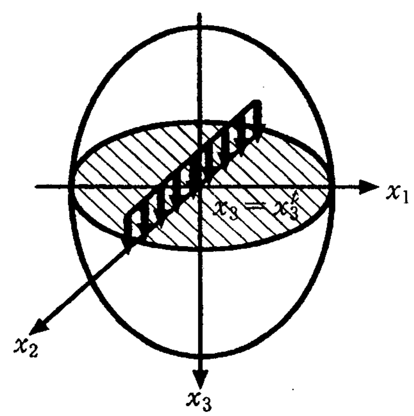

Fig. 1 An applied line load in orthotropic infinite media

defining the orthotropic symmetry is thus coincident with the $x_1 - x_2$ plane. With respect to this coordinate system, the equations of motion in the medium are given by[1]

$$\frac{\partial \sigma_{ij}}{\partial x_i} + f_i = \rho \frac{\partial^2 u_i}{\partial t^2} \tag{1}$$

and, from the general constitutive relations for anisotropic media,

$$\sigma_{ij} = c_{ijkl} e_{kl}, \; i, j, k, l = 1, 2, 3 \tag{2}$$

Where we used the standard contracted subscript notations 1→11, 2→22, 3→33, 4→23, 5→13 and 6→12, to replace fourth order tenser c_{ijkl} $(i, j, k, l = 1, 2, 3)$ with c_{pq} $(p, q = 1, 2, \ldots, 6)$. Thus, c_{45} stands for c_{2313}, for example. Here σ_{ij}, e_{ij} and u_i are the components of stress, strain and displacement, respectively, and ρ is the material density. In Eq. (3), $\gamma_{ij} = 2e_{ij} (i \neq j)$ defines the engineering shear strain components. One would like to solve the case of orthotropic symmetry by applying constitutive Eq. (2) to the secular Eq. (1) that is written in the expanded form in terms of displacement components

$$[c_{11}\frac{\partial^2}{\partial x_1^2} + c_{55}\frac{\partial^2}{\partial x_3^2}]u_1 + (c_{13} + c_{55})\frac{\partial^2 u_3}{\partial x_3^2} = \rho \frac{\partial^2 u_1}{\partial t^2} - f_1 \tag{3a}$$

$$\frac{\partial}{\partial x_3}[(c_{13} + c_{55})\frac{\partial}{\partial x_1}]u_1 + [c_{55}\frac{\partial^2}{\partial x_1^2} + c_{33}\frac{\partial^2}{\partial x_3^2}]u_3 = \rho \frac{\partial^2 u_3}{\partial t^2} - f_3 \tag{3b}$$

$$[c_{66}\frac{\partial^2}{\partial x_1^2} + c_{44}\frac{\partial^2}{\partial x_3^2}]u_2 = \rho \frac{\partial^2 u_2}{\partial t^2} - f_2 \tag{3c}$$

where f_i is defined as $f_1 = f_2 = 0$, $f_3 = Q\delta(x_1)\delta(x_3 - x_3^p)F(t)$. Eq.(2.3c) represents a horizontal shear wave equation that is independent of a vertical shear wave and a longitudinal wave. Since the line load has only vertical component, Eqs.(2.3a,b) need to be considered.

3. Solutions by Fourier transform

Formal solutions are effectuated by applying the Fourier transform to these Eqs.(3a, b) in accordance with

$$\overline{u_q} = \int_0^\infty u_q e^{-pt} dt, \quad \widehat{u_q} = \int_{-\infty}^{\infty} \overline{u_q} e^{-jp\eta x_1} dx_1 \tag{4}$$

The general solution of the resulting differential equations is then sought in the form

$$\widehat{u_i} = U_i e^{-p\alpha x_3}, \quad i = 1, 2, 3 \tag{5}$$

The steps leading to formal solutions of Eqs. (3a,b) for each of the two semi-infinite spaces (See Fig. 1) will be outlined[1]. Body force, f_i, first, is deleted from Eqs. (3a,b), since the body force has been replaced by an "artificial interface conditions", which are given by

$$c_{33}\frac{\partial u_3}{\partial x_3} = -\frac{1}{2}Q\delta(x_1)F(t), \quad \text{for } x_3 \geq x_3^p \text{ at } x_3 = x_3^p$$
$$c_{33}\frac{\partial u_3}{\partial x_3} = \frac{1}{2}Q\delta(x_1)F(t), \quad \text{for } x_3 \leq x_3^p \text{ at } x_3 = x_3^p \tag{6}$$

Infinite Media

The Eqs. (3a,b) lead to the characteristic equation in terms of U_i by substituting Eqs. (4 and 5). The characteristic equation(Christoffel Equation) yields nontrivial solutions in U_i, thereby resulting in the fourth order algebraic equation in α,

$$A_1\alpha^4 + A_2\alpha^2 + A_3 = 0 \tag{7}$$

with its coefficients given by

$$A_1 = c_{33}c_{55}$$
$$A_2 = [(c_{13} + c_{55})^2 - c_{11}c_{33} - c_{55}^2]\eta^2 - (c_{33} + c_{55})\rho$$
$$A_3 = c_{11}c_{55}\eta^4 + (c_{11} + c_{55})\rho\eta^2 + \rho^2 \tag{9}$$

that admits four solutions. The wave amplitude ratio, W_q, is yielded as $-\Lambda_{11}/\Lambda_{13}$ by solving the characteristic equation for α, where Λ_{ij} is given in Appendix. Using superposition, the formal solutions, then, are written for the displacements and their associated stress components as

$$
\begin{aligned}
(\widehat{u}_1, \widehat{u}_3) &= \sum_{q=1}^{4}(1, W_q)U_{1q}e^{-\alpha_q(x_3-x_3^0)} \\
(\widehat{\sigma}_{33}, \widehat{\sigma}_{13}) &= \sum_{q=1}^{4}p(D_{1q}, D_{2q})U_{1q}e^{-\alpha_q(x_3-x_3^0)}
\end{aligned}
\tag{9}
$$

Finally, by applying "artificial interface condition" to Eq. (8), solutions for infinite space can be written in terms of $q=1,3$

$$
\begin{aligned}
2c_{33}D_{uo}\widehat{u}_1\, p &= \overline{F(p)}\,Q[e^{-p\alpha_1|x_3-x_3^0|} - e^{-p\alpha_3|x_3-x_3^0|}] \\
2c_{33}D_{uo}\widehat{u}_3\, p &= \overline{F(p)}\,Q[W_1e^{-p\alpha_1|x_3-x_3^0|} - W_3e^{-p\alpha_3|x_3-x_3^0|}]
\end{aligned}
\tag{10}
$$

where D_{uo} is given in Appendix.

<u>Semi-infinite Media</u>

We now adapt the solutions of the infinite media Eq. (10) to solve for the case where the free boundary intercepts the propagating pulse at some arbitrary location parallel to the plane $x_3=0$. It is assumed that the free boundary is located at $x_3=-d$ as depicted in Fig. 2. This implies that the free boundary is located in the upper region and thus can only interfere with the propagation fields in the negative x_3 direction. For this case, the solution of Eq. (10) will constitute an incident wave on a free surface. As a result, waves will reflect from the free boundary and propagate in the positive x_3 direction. Thus, appropriate formal solutions, superposing the incident waves and the reflected waves, can be adapted from the solution of Eq. (10) in accordance with

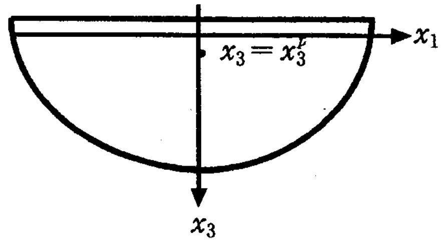

Fig. 2 Semi-infinite media

$$
\begin{aligned}
(\widehat{u_1^s}, \widehat{u_3^s}) &= \sum_{q=1,3}(1, W_q)U_{1q}^r e^{-p\alpha_q x_3} \\
&\quad + \sum_{q=1,3}(-1, W_q)U_{1q}^{(i)} e^{-p\alpha_q(x_3^0-x_3)} \\
(\widehat{\sigma_{33}^s}, \widehat{\sigma_{13}^s}) &= \sum_{q=1,3}(D_{1q}, D_{2q})U_{1q}^r p e^{-p\alpha_q x_3} \\
&\quad + \sum_{q=1,3}(-D_{1q}, D_{2q})U_{1q}^{(i)} p e^{-p\alpha_q(x_3^0-x_3)}
\end{aligned}
\tag{11}
$$

The boundary condition is given by $\widehat{\sigma_{13}^s} = \widehat{\sigma_{33}^s} = 0$ at $x_3=-d$ (12)

By imposing the boundary conditions(12) on Eq. (11), solutions on semi-infinite space are obtained expressible as

$$
\begin{aligned}
\widehat{u_1^s} = \frac{\overline{F(p)}Q}{2c_{33}D_{uo}D_{so}}[\, &\text{sign}\, D_{so}(e^{-p\alpha_3|x_3-x_3^0|} - e^{-p\alpha_1|x_3-x_3^0|}) \\
&+((D_{11}D_{23}+D_{21}D_{13})E_1^r - 2D_{13}D_{23}E_3^r)e^{-p\alpha_1(x_3+d)} \\
&+((D_{11}D_{23}+D_{21}D_{13})E_3^r - 2D_{11}D_{21}E_1^r)e^{-p\alpha_3(x_3+d)}\,]
\end{aligned}
\tag{13a}
$$

$$
\begin{aligned}
\widehat{u_3^s} = \frac{\overline{F(p)}Q}{2c_{33}D_{uo}D_{so}}[\, &D_{so}(W_1e^{-p\alpha_3|x_3-x_3^0|} - W_3e^{-p\alpha_1|x_3-x_3^0|}) \\
&+((D_{11}D_{23}+D_{21}D_{13})E_1^r - 2D_{13}D_{23}E_3^r)W_1e^{-p\alpha_1(x_3+d)} \\
&+((D_{11}D_{23}+D_{21}D_{13})E_3^r - 2D_{11}D_{21}E_1^r)W_3e^{-p\alpha_3(x_3+d)}\,]
\end{aligned}
\tag{13b}
$$

where D_{ij}, and D_{so} are given in Appendix.

4. Cargniard-DeHoop Contour Variation

Now transformations $\widehat{u_q}$ will be back to the time-space domain by using Cargniard DeHoop method. The method is based on the following elementary property of the one-sided Laplace transform:

For a given Laplace transforms,

$$\overline{u_i} = \int_{t_q}^{\infty} u_i\ (x_1, x_3, t)e^{-pt}\, dt$$

The inverse of the integral is

$$u_i = u_i(x_1, x_3, t),\ \ \mathrm{H}(t-t_q)$$

where $\mathrm{H}(t-t_q)$ is the Heavyside step function. First, consider the Laplace transform of u_i. $\overline{u_i}$ is obtained by

$$2\pi \overline{u_i} = \int_{-\infty}^{\infty} U_{11} e^{-p(\alpha_1 x_3 - j\eta x_1)} d\eta + \int_{-\infty}^{\infty} U_{13} e^{-p(\alpha_3 x_3 - j\eta x_1)} d\eta \quad (14)$$

The integration in the complex η-plane is carried out along the (four different) paths

$$\text{where} \quad t = \alpha x_3 - j\eta x_1 \quad \text{or} \quad \alpha = \frac{t + j\eta x_1}{x_3} \quad (15)$$

with t real and positive. Substitution of (5) into the characteristic Eq. (10) yields the fourth order polynomial defining the Fourier parameter η :

$$\Omega(x_1, x_3, t, \eta) = B_4\eta^4 + B_3\eta^3 + B_2\eta^2 + B_1\eta + B_0 = 0 \quad (16)$$

where B_i is given in Appendix. The four root is composed of two parabolas with respect to time t for a certain position (x_1, x_3), and they are symmetric about the imaginary η axis. Each of the parabolas is associated with four distinct roots of α from the characteristic Eq. (7), two of which correspond to the lower half-space and others to the upper half-space, because of the boundedness of the wave. Each of the two η represents a separate wavefront.

Infinite Media

Now the inverse Laplace transform can be obtained by mere inspection of Eq. (10)

$$\frac{4\pi c_{33}}{Q} u_1 = \left[\frac{1}{D_{uo}(\eta_1^+)}\frac{\partial\eta_1^+}{\partial t} - \frac{1}{D_{uo}(\eta_1^-)}\frac{\partial\eta_1^-}{\partial t}\right] H(t-t_1) - \left[\frac{1}{D_{uo}(\eta_2^+)}\frac{\partial\eta_2^+}{\partial t} - \frac{1}{D_{uo}(\eta_2^+)}\frac{\partial\eta_2^-}{\partial t}\right] H(t-t_2) \quad (17a)$$

$$\frac{4\pi c_{33}}{Q} u_3 = \left[\frac{W_3(\eta_1^+)}{D_{uo}(\eta_1^+)}\frac{\partial\eta_1^+}{\partial t} - \frac{W_1(\eta_1^-)}{D_{uo}(\eta_1^-)}\frac{\partial\eta_1^-}{\partial t}\right] H(t-t_1) - \left[\frac{W_3(\eta_2^+)}{D_{uo}(\eta_2^+)}\frac{\partial\eta_2^+}{\partial t} - \frac{W_1(\eta_2^+)}{D_{uo}(\eta_2^+)}\frac{\partial\eta_2^-}{\partial t}\right] H(t-t_2) \quad (17b)$$

and

$$\frac{\partial\eta_i}{\partial t} = -\frac{\partial\Omega}{\partial\eta} / \frac{\partial\Omega}{\partial t} = [4B_4\eta^3 + 3B_3\eta^2 + 2B_2\eta + B_1\eta] \div [4D_1t^3 + 12jD_1x_1t^2 - 2(6D_1x_1^2 - (D_3 - D_2)x_3^2)t - 2jx_1(2D_1x_1^2 + (2D_3 - D_2)x_3^2)] \quad (18)$$

where D_i is given in Appendix. The t_1 and t_2 are the arrival times of the wave fronts. In other words, they are the times that correspond to the values of the imaginary η^- axis intercepts of the two branches of η. The notation η^+ denotes the branch of η_i to the right side of the imaginary η axis and η^- denotes the branch of η_i to the left side of the imaginary η axis.

Semi-Infinite Media

By the same procedure, integral transform solutions of Eq.(13a,b) in the semi-infinite media are inversely transformed back to the space-time domain. The result of the wave propagation is given by

$$\frac{4\pi c_{33}}{Q} u_1^s = \left[\frac{D_{uo}D_{so} + D_{11}D_{23} + D_{21}D_{13} - 2D_{11}D_{21}}{D_{uo}D_{so}}(\eta_1^+)\frac{\partial\eta_1^+}{\partial t} - \frac{D_{uo}D_{so} + D_{11}D_{23} + D_{21}D_{13} - 2D_{11}D_{21}}{D_{uo}D_{so}}(\eta_1^+)\frac{\partial\eta_1^+}{\partial t}\right] H(t-t_1) - \left[\frac{D_{uo}D_{so} + D_{11}D_{23} + D_{21}D_{13} - 2D_{13}D_{23}}{D_{uo}D_{so}}(\eta_2^+)\frac{\partial\eta_2^+}{\partial t} - \frac{D_{uo}D_{so} + D_{11}D_{23} + D_{21}D_{13} - 2D_{13}D_{23}}{D_{uo}D_{so}}(\eta_2^+)\frac{\partial\eta_2^+}{\partial t}\right] H(t-t_2) \quad (19)$$

The remaining displacement u_3^s will be optained by the same procedures.

6. Numerical Illustration and Discussion

Numerical illustrations are presented for the analysis. An InAs cubic material is chosen and its material constants are given by $c_{11}=c_{22}=c_{33}=83.29\times10^{10}\ \mathrm{N/m^2}$, $c_{12}=c_{13}=c_{23}=45.26\times10^{10}\ \mathrm{N/m^2}$, $c_{44}=c_{55}=c_{66}=39.59\times10^{10}\ \mathrm{N/m^2}$ and $\rho=5.67\ \mathrm{g/cm^3}$ Fig. 3(a) represents the imaginary part of η variation with respect to time t along the wave propagating direction of 10° with respect to x_3 axis on x_1-x_3 plane. t_1, t_2, t_3 and t_4 in Fig. 3(b) ~3(c) are assigned for the arrival times of various wave forms in displacement field, u and w. The sharp jerks are due to the nature of the direc delta function of the line load. All displacements vanish at $t_2 \le t \le t_3$, which represents anisotropy degeneracy of the material. Fig. 4 presents snap shot of absolute value of radical displacement field at fixed time (t =0.2usec). A spatial grid of 100x100 points is generated for the first quadrant. The remaining quadrants are then generated by the mirror of the first quadrant. The vertical line load is located at the origin that is the center of the picture. Since the medium is homogeneous, the wave field does not change as it propagates. The color scheme runs from white (minimum) to black (maximum). In this picture we can clearly recognize the wave curves (three wave fronts and lacunae). The picture shows that the contribution of the longitudinal wave is strong at $\vartheta=0^{\circ}$ whereas that of the shear wave is strong at $\vartheta=90^{\circ}$. Fig. 5 presents snap shot of absolute value of radical displacement field at fixed time (t =0.2usec). The material properties are given as $c_{11}=c_{22}=c_{33}=278.74\times10^{10}\ \mathrm{N/m^2}$, $c_{12}=c_{13}=c_{23}=33.0\times10^{10}$

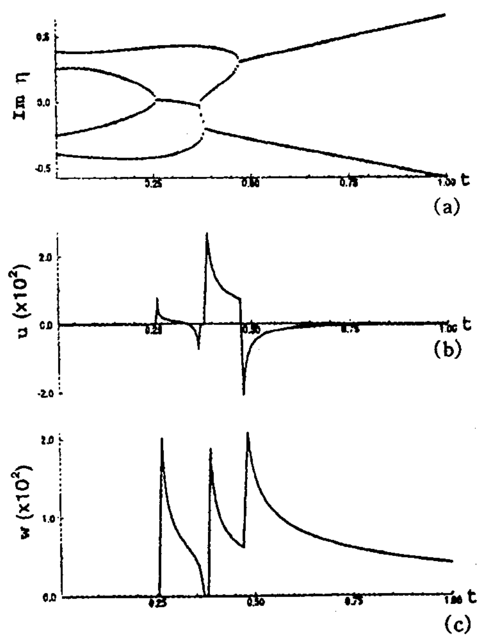

Fig. 3 Various responses due to a line load in the cubic medium of InAs
(a) Imaginary part of η variation versus time (μsec)
(b) Horizontal displacement u versus time
(c) Vertical displacement w versus time

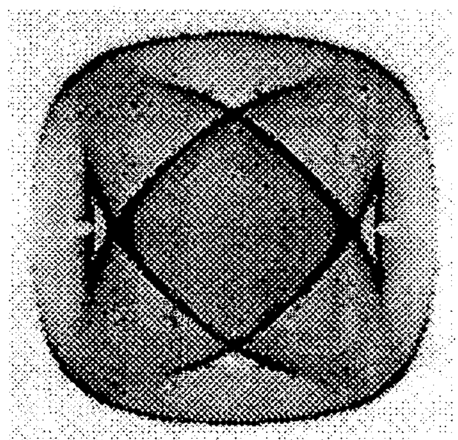

Fig. 4 Snap shot of displacement field at t =0.2μsec of InAs infinite system

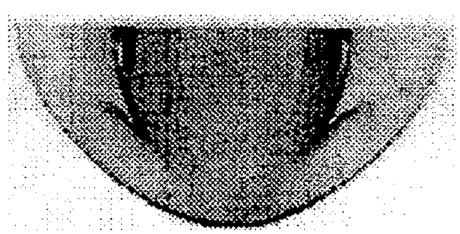

Fig. 5 Snap shot of displacement field at t =0.2μsec of semi-infinite system

N/m^2, $c_{44}=c_{55}=c_{66}=81.91\times10^{10}\,N/m^2$ and $\rho=1.7\,g/cm^3$. In this figure, we can clearly recognize the wave curves (surface wave and two bulk wave forms). The surface wave peaks are shown at inside of the longitudinal wave front and near the horizontal plane surface.

7. Conclusion

Explicit solutions for the displacements due to transient line loads, which include infinite, semi-infinite spaces, are obtained by using Cargniard-DeHoop contour. Numerical results which are drawn from concrete examples of orthotropic symmetry are demonstrated. These analytical solutions are adquate for the material system possessing orthotropic or higher symmetry, transversely isotropic, cubic, and isotropic symmetry. The solutions of the system with orthotropic symmetry will be simplified to those of isotropic systems by exploiting elastic properties of λ and μ.

References

(1) Y. Y. Kim, 1993, "Elastic Waves in Anisotopic Media," Ph.D. Dissertation, University of Cincinnati.

(2) D. E. Chimenti and A. H. Nayfeh, 1990, "Ultrasonic Reflection and Guided Waves in Fluid-Coupled omposite Laminates", J. Non-Structive Evaluation, Vol. 9, No. 2/3.

(3) A. H. Nayfeh and D. E. Chimenti, 1988, "Propagation of Guided Waves in Fluid-Coupled Composite Plates of Fiber-Reinforced Composites", J. Appl. Mech., Vol. 83, pp. 1736.

(4) D. E. Chimenti and A. H. Nayfeh, 1989, "Ultrasonic Leaky Waves in a Solid Plate Separating Fluid and Vacuum Media", J. Acous. Soc. Am., Vol. 85, p. 2.

(5) J. P. Achenbach, 1973, Wave Propagations in Elastic Solids, American Elsevier Pub. Co., New York.

(6) Y. C. Fung, Foundation of Solid Mechanics, 1965, Prentice-Hall, Englewood Cliffs, N. J.

(7) A. T. De Hoop, 1960, "A Modification of Cargniard's Method for Solving Seismic Pulse Problems", Appli.sci.Res., B, Vol. 8 pp. 349~357.

(8) W. Ewing, W. Jardetzky and F. Press, 1957, Elastic Media, McGraw Hill, New York.

(9) G. Eason, J. Fulton and I. N. Sneddon, 1956, "The Generation of Wave in an Infinite Elastic Solid by Variable Body Forces", Phil. Trans. Roy. Soc., London, Ser. A, Vol. 248, pp. 575~308.

(10) E. R. Lapwood, 1949, "The Disturbance Due to a Line Source in a Semi-infinite Elastic Edium", Phil. Trans. Roy. Soc., London, Ser. A, Vol. 242, pp. 9~100.

(11) H. Lamb, 1917, "On Waves in an Elastic Plate", Phil. Trans. Roy. Soc., London, Ser. A, Vol. 93, pp. 124~128.

(12) Lord Rayleigh, 1889, "On the Free Vibrations of an Infinite Plate of Homogeneous Isotropic Elastic Material, Proc. London Mathematical Society, 20, p. 225.

Appendix

Various coefficients are given by

$$\Lambda_{11}=c_{55}\alpha^2-c_{11}\eta^2-\rho$$
$$\Lambda_{13}=-j\eta\alpha(c_{13}+c_{55})$$
$$\Lambda_{33}=c_{33}\alpha^2-c_{55}\eta^2-\rho$$
$$D_{1q}=j\eta c_{13}-c_{33}\alpha_q W_q$$
$$D_{2q}=c_{55}(j\eta W_q-\alpha_q)$$
$$D_{uo}=\alpha_1 W_1-\alpha_3 W_3$$
$$D_{so}=D_{11}D_{23}-D_{21}D_{13}$$
$$B_0=D_1t^4-D_3x_3^2t^2+\rho^2x_3^4$$
$$B_1=j(4D_1x_1t^3-2D_3x_1x_3^2t^2)$$
$$B_2=(D_2x_3^2-6D_1x_1^2)t^2+(D_3x_1^2+D_4x_3^2)x_3^2$$
$$B_3=j(2D_2x_1x_3^2-4D_1x_1^3)t$$
$$B_4=D_1x_1^4-D_2x_1^2x_3^2+D_4x_3^4$$
$$D_1=c_{33}c_{55}$$
$$D_2=c_{13}^2+2c_{13}c_{55}-c_{11}c_{33}$$
$$D_3=-\rho(c_{33}+c_{55})$$
$$D_4=c_{11}c_{55}$$
$$D_5=\rho(c_{11}+c_{55})$$